

Analytical and Numerical Investigations for the Flow and Heat Transfer of Nanofluids over a Stretching Sheet with Partial Slip Boundary Condition

Emad H. Aly^{1,2,*}, Abdelhalim Ebaid³ and Nader Y. Abd Elazem³

¹ Department of Mathematics, Faculty of Science, King Abdulaziz University, Jeddah 21589, Saudi Arabia

² Department of Mathematics, Faculty of Education, Ain Shams University, Roxy 11757, Cairo, Egypt

³ Department of Mathematics, Faculty of Science, University of Tabuk, Tabuk 71491, Saudi Arabia

Received: 20 Jul. 2013, Revised: 22 Oct. 2013, Accepted: 23 Oct. 2013

Published online: 1 Jul. 2014

Abstract: Due to importance of the slip effect on modeling the boundary layer flows of nanofluids, theoretical and numerical investigations have been introduced in this paper for studying the effect of a partial slip boundary condition on the heat transfer of nanofluids over a stretching sheet. The exact solutions of the investigating model were obtained in terms of exponential, Gamma, and incomplete Gamma functions at some values of the physical parameters. These solutions were then numerically validated by using Chebyshev pseudospectral differentiation matrix (ChPDM) technique. The numerical results reveal that this approach is really effective, very accurate, and convenient in studying the similar problems.

Keywords: Nanofluid; stretching sheet; partial slip; heat transfer; exact solution; ChPDM

1 Introduction

In the recent times, the study of fluid flow over a stretching sheet has gained much interest because of its numerous industrial applications for example, in the polymer processing of a chemical engineering plant and in metallurgy. Flows due to a continuously moving surface are encountered in several processes of thermal and moisture treatment of materials, predominantly in processes involving continuous pulling of a sheet through a reaction zone; as in metallurgy, in textiles and paper industries, and in the manufacture of glass sheets and crystalline materials. In addition, nanotechnology is nowadays considered as a significant factor which affects the industrial revolution of the current century. Nanofluids are base-fluids containing suspended nanoparticles. These nanoparticles are typically made of metals, oxides, carbides, or carbon nanotubes. The common base fluids include water, ethylene glycol, toluene and oil. Therefore, many researchers have focused on modeling the thermal conductivity and examined different viscosities of nanofluids over the past decade, etc ([1], [2], [3]).

Choi [4] may be the first author to use the term “nanofluid”, where it was reported that one of the promising nanofluids applications is heat transfer enhancement. In [5], Choi et al. showed that the addition of a small amount (less than 1% by volume) of nanoparticles to conventional heat transfer liquids increased the thermal conductivity of the fluid up to approximately two times. Masuda et al. [6], Lee et al. [7], Xuan and Li [8], and Xuan and Roetzel [9] stated that with low nanoparticles concentrations (1–5 Vol %), the thermal conductivity of the suspensions can increase more than 20%. Such an increase depends mainly on several factors such as the form and size of the particles and their concentration, the thermal properties of the base-fluid as well as those of the particles. Hence, the nanofluids can constitute an interesting alternative for advanced applications in heat transfer in the future, especially those in micro scale, see for example [7].

Recently, some interest has been given to the study of the boundary layer flow of nanofluids past a stretching sheet. In [10], Nield and Kuznetsov discussed the Cheng–Minkowycz problem for natural convective boundary layer flow in a porous medium saturated by a

* Corresponding author e-mail: emad-aly@hotmail.com

nanofluid. Besides, Kuznetsov and Nield [11] investigated the natural convective boundary-layer flow of a nanofluid past a vertical plate. Further attempts in this direction have been done by Khan and Pop [12] and later in the same year by Bachok et al. [13] who studied the steady boundary layer flow of a nanofluid past a moving semi-infinite flat plate. Very recently, the model obtained in [12] has been solved theoretically by Aly and Ebaid [14], where exact solutions at several particular values of the physical parameters have been reported. However, the slip effect at the wall was ignored in all of the previous studies.

It has been shown in [15] that nanofluidic flow usually exhibits partial slip against the solid surface, which can be characterized by the so-called slip length (around 3.4–68 nm for different liquids). Accordingly, Noghrehabada et al. [16] discussed the effect of partial slip boundary condition on the flow and heat transfer of nanofluids past stretching sheet at constant wall temperature. Furthermore, the no-slip condition is no longer valid for fluid flows at the micro and nano scale and, instead, a certain degree of tangential slip must be allowed (see for example [17] and [18]).

The objective of the present research is therefore to extend the work of Noghrehabada et al. [16], stated in Section 2, where new analytical and numerical results are deduced at some values of the investigating physical parameters. In general, it is shown that the current exact solutions are obtained in the view of exponential, Gamma and incomplete Gamma functions with a simple but very effective manner. They are then validated and plotted by using Chebyshev pseudospectral differentiation matrix (ChPDM) approach, introducing briefly in Section 3. Moreover, it is proved that the exact analytical solutions of the present study can be easily reduced to those obtained in [14] when the slip factor finishes.

2 The studying model

In this paper, we focus on the physical model derived by Noghrehabadi et al. [16] and given by

$$f'''(\eta) + f(\eta)f''(\eta) - [f'(\eta)]^2 = 0, \quad (1)$$

$$\frac{1}{Pr} \theta''(\eta) + f(\eta)\theta'(\eta) + Nb \beta'(\eta)\theta'(\eta) + Nt [\theta'(\eta)]^2 = 0, \quad (2)$$

$$\beta''(\eta) + Le f(\eta)\beta'(\eta) + \frac{Nt}{Nb} \theta''(\eta) = 0, \quad (3)$$

subject to the following boundary conditions:

$$f(0) = 0, f'(0) = 1 + \lambda f''(0), \theta(0) = 1, \beta(0) = 1, \quad (4)$$

$$f'(\infty) = 0, \theta(\infty) = 0, \beta(\infty) = 0, \quad (5)$$

where f , θ and β are the dimensionless of the stream function, temperature and nanoparticle volume fraction, respectively. Further, primes denote to differentiation with respect to the similarity variable η and Pr , Le , Nb , Nt and

λ are the Prandtl number, Lewis number, Brownian motion parameter, thermophoresis parameter and slip factor, respectively. When $\lambda = 0$, i.e. with no effect of the slip parameter, the system (1)–(5) is reduced to that one obtained in [12]. In addition, the exact solution of Eq. (1) with the boundary conditions in (4)–(5) can be easily found as ([19]–[20])

$$f(\eta) = \varepsilon (1 - e^{-\varepsilon\eta}), \quad \text{where } \lambda \varepsilon^3 + \varepsilon^2 - 1 = 0, \quad (6)$$

where ε is the maximal root of the equation. By Descartes' rule of signs and from the fact that $\lambda > 0$, there is only one positive root; this is the root to be considered [18]. Therefore, the given system reduces to the following set of ordinary differential equations:

$$\frac{1}{Pr} \theta'' + [\varepsilon (1 - e^{-\varepsilon\eta}) + Nb \beta'] \theta' + Nt [\theta']^2 = 0, \quad (7)$$

$$\beta'' + Le \varepsilon (1 - e^{-\varepsilon\eta}) \beta' + \frac{Nt}{Nb} \theta'' = 0, \quad (8)$$

where the boundary conditions on $\theta(\eta)$ and $\beta(\eta)$ are given in Eqs. (4) and (5). According to Kuznetsov and Nield [11], the quantities of practical interest are the reduced Nusselt number (Nur) and reduced Sherwood number (Shr) which are defined by

$$Nur = -\theta'(0), \quad Shr = -\beta'(0). \quad (9)$$

3 ChPDM approach

Chebyshev pseudospectral differentiation matrix (ChPDM) technique was applied successfully by Aly et al. [21], Guedda et al. [22], Aly and Ebaid ([19], [23]) and Aly and Hassan [24]. It is briefly introduced here. On supposing that the domain of the problem is $[0, \eta_\infty]$, then the following algebraic mapping

$$z = \frac{2\eta}{\eta_\infty} - 1 \quad (10)$$

transfers the domain to the Chebyshev one, i.e. $[-1, 1]$. It is known that the Chebyshev polynomials are usually taken with their associated collocation points in the interval $[-1, 1]$ given by

$$z_j = \cos\left(\frac{\pi}{N}j\right), \quad j = 0, 1, \dots, N. \quad (11)$$

Therefore, the k^{th} derivative of any function, say $\mathbf{F}(z)$, at these collocation points can be approximated by the equation:

$$\mathbf{F}^{(k)} = D^{(k)} \mathbf{F}, \quad (12)$$

where $D^{(k)} \mathbf{F}$ is the Chebyshev pseudospectral approximation of $\mathbf{F}^{(k)}$ where

$$\mathbf{F} = [F(z_0), F(z_1), \dots, F(z_N)]^T \quad \text{and}$$

$\mathbf{F}^{(k)} = [F^{(k)}(z_0), F^{(k)}(z_1), \dots, F^{(k)}(z_N)]^T$. The entries of the matrix $D^{(k)}$ are given by,

$$d_{i,j}^{(k)} = \frac{2\phi_j}{N} \sum_{r=k}^N \sum_{\substack{n=0 \\ (n+r-k) \text{ even}}}^{r-k} \phi_r b_{n,r}^k (-1)^{\lfloor \frac{rj+ni}{N} \rfloor} z_{rj-N\lfloor \frac{rj}{N} \rfloor} z_{ni-N\lfloor \frac{ni}{N} \rfloor}, \quad (13)$$

where $\phi_j = 1$, except for $\phi_0 = \phi_N = \frac{1}{2}$ and

$$b_{n,r}^k = \frac{2^k r}{(k-1)! c_n} \frac{(v-n+k-1)! (v+k-1)!}{(v)! (v-n)!}, \quad (14)$$

where $2v = r + n - k$ and $c_0 = 2$, $c_j = 1$, $j \geq 1$. The elements $d_{0,1}^{(k)}$ are the major elements concerning its values. Accordingly, they bear the major error responsibility comparing the other elements. It is shown that the error in $d_{0,1}^{(1)}$ is of order $O(N^2 \epsilon_r)$, where ϵ_r is the machine precision [25].

On the view of Refs. [21] to [24], on applying ChPDM approach; derivatives of the function $f(\eta)$, $\theta(\eta)$ and $\beta(\eta)$ at the points z_i are given by

$$\chi^{(k)}(z_i) = \sum_{j=0}^N d_{i,j}^{(k)} \chi(z_j), \quad \chi \equiv f, \theta, \beta, k = 1, 2, 3, i = 1, 2, \dots, N. \quad (15)$$

Therefore, Eqs. (1)–(5) become

$$\sum_{j=0}^N d_{i,j}^{(3)} f(z_j) + f(z_i) \left(\frac{\eta_\infty}{2} \right) \sum_{j=0}^N d_{i,j}^{(2)} f(z_j) - \left(\frac{\eta_\infty}{2} \right) \left(\sum_{j=0}^N d_{i,j}^{(1)} f(z_j) \right)^2 = 0. \quad (16)$$

$$\begin{aligned} \frac{1}{Pr} \sum_{j=0}^N d_{i,j}^{(2)} \theta(z_j) + f(z_i) \left(\frac{\eta_\infty}{2} \right) \sum_{j=0}^N d_{i,j}^{(1)} \theta(z_j) \\ + Nb \sum_{j=0}^N d_{i,j}^{(1)} \beta(z_j) \sum_{j=0}^N d_{i,j}^{(1)} \theta(z_j) \\ + Nt \left(\sum_{j=0}^N d_{i,j}^{(1)} \theta(z_j) \right)^2 = 0. \end{aligned} \quad (17)$$

$$\begin{aligned} \sum_{j=0}^N d_{i,j}^{(2)} \beta(z_j) + Le f(z_i) \left(\frac{\eta_\infty}{2} \right) \sum_{j=0}^N d_{i,j}^{(1)} \beta(z_j) \\ + \frac{Nt}{Nb} \sum_{j=0}^N d_{i,j}^{(2)} \theta(z_j) = 0. \end{aligned} \quad (18)$$

$$f(z_N) = 0,$$

$$\left(\frac{\eta_\infty}{2} \right) \sum_{j=0}^N d_{N,j}^{(1)} f(z_j) = \left(\frac{\eta_\infty}{2} \right)^2 + \lambda \sum_{j=0}^N d_{N,j}^{(2)} f(z_j), \quad (19)$$

$$\theta(z_N) = 1, \quad \beta(z_N) = 1,$$

$$\sum_{j=0}^N d_{0,j}^{(1)} f(z_j) = 0, \quad \theta(z_0) = 0, \quad \beta(z_0) = 0, \quad (20)$$

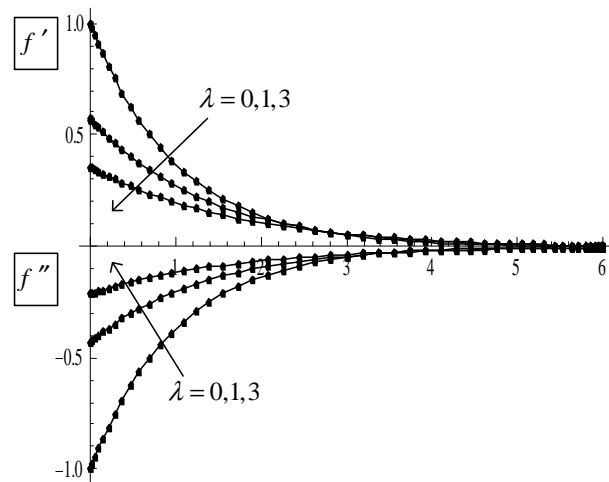


Fig. 1: Comparison of ChPDM (solid lines) and Runge-Kutta-Fehlberg scheme (circles) [16] solutions for $f'(\eta)$ and $f''(\eta)$ at $\lambda = 0, 1, 3$, $Pr = Le = 10$ and $Nb = Nt = 0.5$.

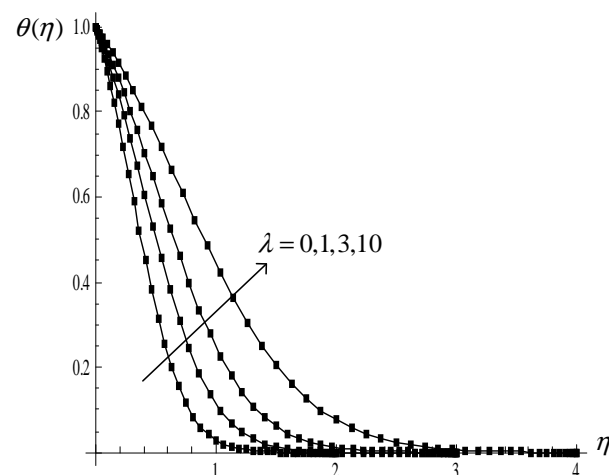


Fig. 2: ChPDM (solid line) and Runge-Kutta-Fehlberg scheme (circles) [16] solutions for $\theta(\eta)$ at $\lambda = 0, 1, 3, 10$, $Pr = Le = 10$ and $Nb = Nt = 0.1$

respectively.

Before starting the current analysis, ChPDM technique is applied by using the system (16)–(20). Figs. 1, 2 and 3(a) and (b) show the comparison between ChPDM and Runge-Kutta-Fehlberg scheme [16] for the solutions of $f'(\eta)$ and $f''(\eta)$, $\theta(\eta)$ and $\beta(\eta)$, respectively, for various values of the investigated parameters. As shown, these figures are very close to Figs. 2, 3 and 4, respectively, given in [16]. Hence, without any hesitation, ChPDM technique may be applied with highly trust in the next section.

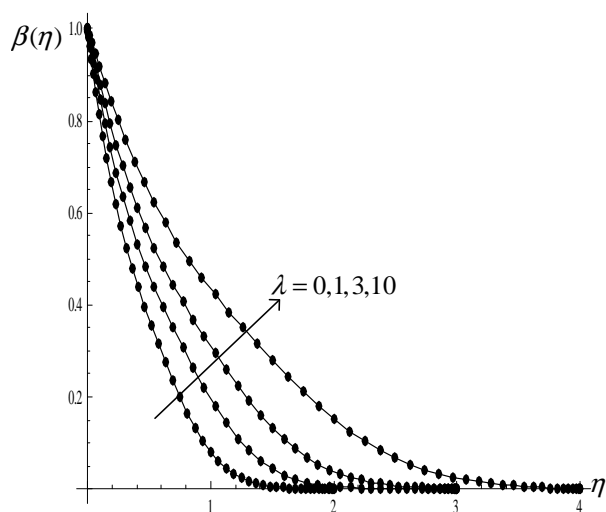


Fig. 3: ChPDM (solid line) and Runge-Kutta-Fehlberg scheme (circles) [16] solutions for $\beta(\eta)$ at $\lambda = 0, 1, 3, 10$, $Pr = Le = 10$ and $Nb = Nt = 0.1$.

4 Exact solutions for special cases at $Nt = 0$

The possibility of obtaining exact solutions for the present governing equations, i.e. the system (1)–(5), at several particular values of the physical parameters are introduced in this section with validating them by using the ChPDM approach. In addition, it is proved that the results obtained by Aly and Ebaid [14] are a special case of the present ones when there is no effect of the slip parameter, i.e. at $\lambda = 0$.

4.1 Case 1: at $Nb \neq 0$

At $Nt = 0$, the system (7)–(8) reduces to two coupled ordinary differential equations:

$$\theta''(\eta) + Pr [\varepsilon (1 - e^{-\varepsilon\eta}) + Nb\beta'(\eta)] \theta'(\eta) = 0, \quad (21)$$

$$\beta''(\eta) + Le \varepsilon (1 - e^{-\varepsilon\eta}) \beta'(\eta) = 0, \quad (22)$$

On integrating Eq. (22) twice w.r.t. η and using the boundary conditions (4–5) we obtain

$$\beta(\eta) = 1 + e^{Le} \beta'(0) \int_0^\eta e^{-\varepsilon Le [\sigma + \frac{1}{\varepsilon} e^{-\varepsilon\sigma}]} d\sigma. \quad (23)$$

On using the assumption $\mu = Le e^{-\sigma}$, the last integration can be analytically performed in the terms of Gamma and

incomplete Gamma functions as follows:

$$\begin{aligned} & \int_0^\eta e^{-\varepsilon Le [\sigma + \frac{1}{\varepsilon} e^{-\varepsilon\sigma}]} d\sigma \\ &= \frac{1}{\varepsilon} (Le)^{-Le} \int_{Le e^{-\varepsilon\eta}}^{Le} \mu^{Le-1} e^{-\mu} d\mu \\ &= \frac{1}{\varepsilon} (Le)^{-Le} \left[\int_{Le e^{-\varepsilon\eta}}^\infty \mu^{Le-1} e^{-\mu} d\mu - \int_{Le}^\infty \mu^{Le-1} e^{-\mu} d\mu \right] \\ &= \frac{1}{\varepsilon} (Le)^{-Le} [\Gamma(Le, Le e^{-\varepsilon\eta}) - \Gamma(Le, Le)], \end{aligned} \quad (24)$$

where $\Gamma(a, z) = \int_z^\infty \mu^{a-1} e^{-\mu} d\mu$ is the incomplete Gamma function. Substituting (24) into Eq. (23), it then results

$$\beta(\eta) = 1 + \frac{1}{\varepsilon} (e/Le)^{Le} \beta'(0) [\Gamma(Le, Le e^{-\varepsilon\eta}) - \Gamma(Le, Le)]. \quad (25)$$

Applying the boundary condition $\beta(\infty) = 0$, we get

$$\frac{1}{\varepsilon} (e/Le)^{Le} \beta'(0) = \frac{-1}{\Gamma(Le) - \Gamma(Le, Le)}. \quad (26)$$

On inserting (26) into (25), we obtain $\beta(\eta)$ in an exact form as

$$\beta(\eta) = \frac{\Gamma(Le) - \Gamma(Le, Le e^{-\varepsilon\eta})}{\Gamma(Le) - \Gamma(Le, Le)}. \quad (27)$$

It should be noted that when $\varepsilon = 1$, i.e. at $\lambda = 0$ (no effect of the slip factor), Eq. (27) reduces to that special case in [14]. Inserting (27) into (21) and repeating the same analysis made above, we obtain $\theta(\eta)$ in a closed analytical form as

$$\begin{aligned} \theta(\eta) &= 1 - \frac{I(\eta)}{I(\infty)}, \\ I(\eta) &= \int_0^\eta e^{-Pr \left[\varepsilon \left(\sigma + \frac{e^{-\varepsilon\sigma}}{\varepsilon} \right) + Nb \left(\frac{\Gamma(Le) - \Gamma(Le, Le e^{-\varepsilon\eta})}{\Gamma(Le) - \Gamma(Le, Le)} \right) \right]} d\sigma \end{aligned} \quad (28)$$

According to (9), the exact values of Nur and Shr numbers are given by

$$Nur = \frac{e^{-Pr(1+Nb)}}{I(\infty)}, \quad Shr = \frac{\varepsilon (Le/e)^{Le}}{\Gamma(Le) - \Gamma(Le, Le)}. \quad (29)$$

Fig. 4 shows comparison of the exact and numerical solutions for $\beta(\eta)$ at different values of $Nb = 0.1, 0.2, 0.3, 0.4, 0.5$ when $\lambda = 1$ and $Pr = Le = 10$. This figure indicates that there is no effect of Nb and is clearly matching with Eq. (27), where Nb is not exist. Therefore, the value of Nb is considered as 0.1 in the rest of this section.

Exact and numerical solutions for $\beta(\eta)$ at different values of $\lambda = 0, 1, 3, 5, 10$ when $Nb = 0.1$ and $Pr = Le = 10$ are plotted in Fig. 5, which shows a very good agreement between these two types of solutions. In addition, as expecting from [16], the profiles of $\beta(\eta)$ increase with the increase in λ .

Profiles of $\beta(\eta)$ in the exact and numerical view at different values of $Le = 1, 3, 10, 15, 25$ when $Nb = 0.1$

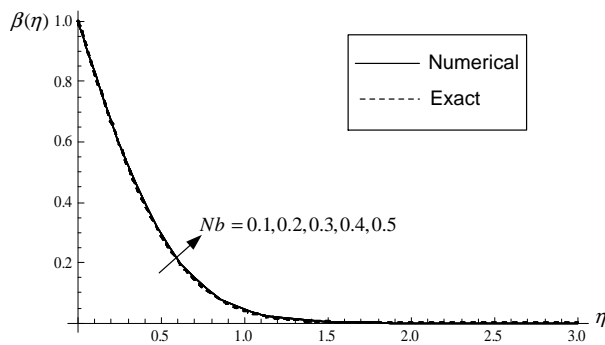


Fig. 4: Exact (dotted line) and numerical (solid line) solutions for $\beta(\eta)$ at $Nb = 0.1, 0.2, 0.3, 0.4, 0.5$ when $\lambda = 1$ and $Pr = Le = 10$.

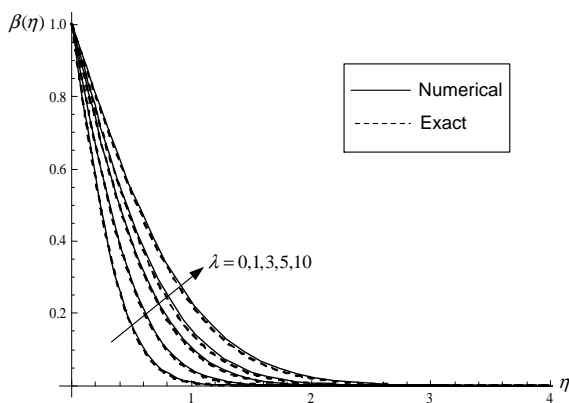


Fig. 5: Exact (dotted line) and numerical (solid line) solutions for $\beta(\eta)$ at $Nb = 0.1$, $\lambda = 0, 1, 3, 5, 10$ and $Pr = Le = 10$.

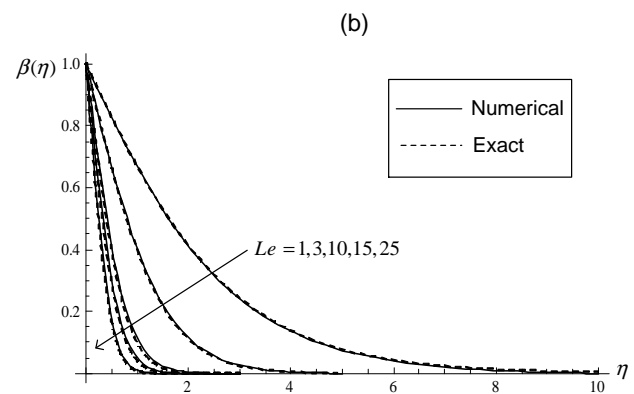
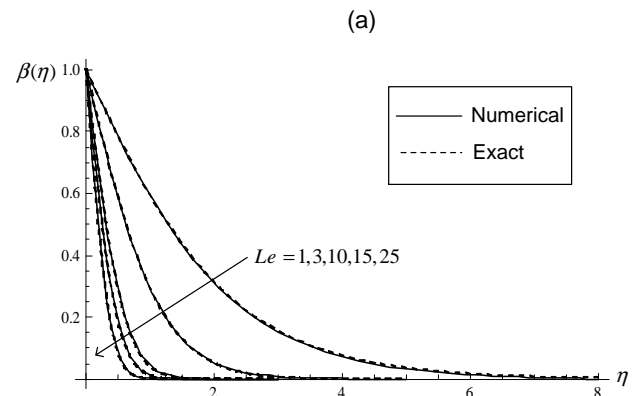


Fig. 6: Exact (dotted line) and numerical (solid line) solutions for $\beta(\eta)$ at $Nb = 0.1$, $Pr = 10$ and $Le = 1, 3, 10, 15, 25$ for (a) $\lambda = 1$ and (b) $\lambda = 3$.

and $Pr = 10$ are presented in Fig. 6 for (a) $\lambda = 1$ and (b) $\lambda = 3$. Besides the typical matching of the exact and numerical solutions at the specific value of λ , these profiles decrease with the increase in Le . However, η_∞ increase with the increase in λ .

4.2 Case 2: at $Nb \neq 0$ and $Pr = Le = 1$

In this case a simpler exact expression for $\beta(\eta)$ is given below

$$\beta(\eta) = \delta \left(1 - e^{-\varepsilon\eta}\right), \quad \text{where} \quad \delta = (1 - e^{-1})^{-1}. \quad (30)$$

In order to determine $\theta(\eta)$, the integral in (28) should be first performed. By inserting $Pr = Le = 1$ into $I(\eta)$ defined in (28), yields

$$I(\eta) = \frac{1}{\varepsilon\delta Nb} \left[e^{-Nb\beta(\eta)} - e^{-Nb} \right], \quad (31)$$

$$I(\infty) = \frac{1}{\varepsilon\delta Nb} \left[1 - e^{-\varepsilon Nb} \right]. \quad (32)$$

Therefore

$$\theta(\eta) = \frac{1 - e^{-Nb\beta(\eta)}}{1 - e^{-Nb}}. \quad (33)$$

Here, the exact values of Nur and Shr numbers are given respectively by

$$Nur = \frac{\varepsilon\delta Nb e^{-(1+Nb)}}{1 - e^{-Nb}}, \quad Shr = \frac{\varepsilon}{e - 1}. \quad (34)$$

The results in this section are again the same ones that obtained in [14] when $\varepsilon = 1$, i.e. at $\lambda = 0$.

Fig. 7(a, b) shows the comparison of $\beta(\eta)$ and $\theta(\eta)$ in the exact (dotted line) and numerical (solid line) view at different values of $\lambda = 0, 1, 3, 10$ when $Le = Pr = 1$ for (a) $Nb = 0.1$ and (b) $Nb = 0.5$. In addition to the typical matching of these two type of solutions at the specific value of λ , these profiles increase with the increase in λ . It should be also noted that $\beta(\eta)$ and $\theta(\eta)$ behave in the same manner. However, $\theta(\eta) > \beta(\eta)$ with a slightly bigger difference at $Nb = 0.5$.

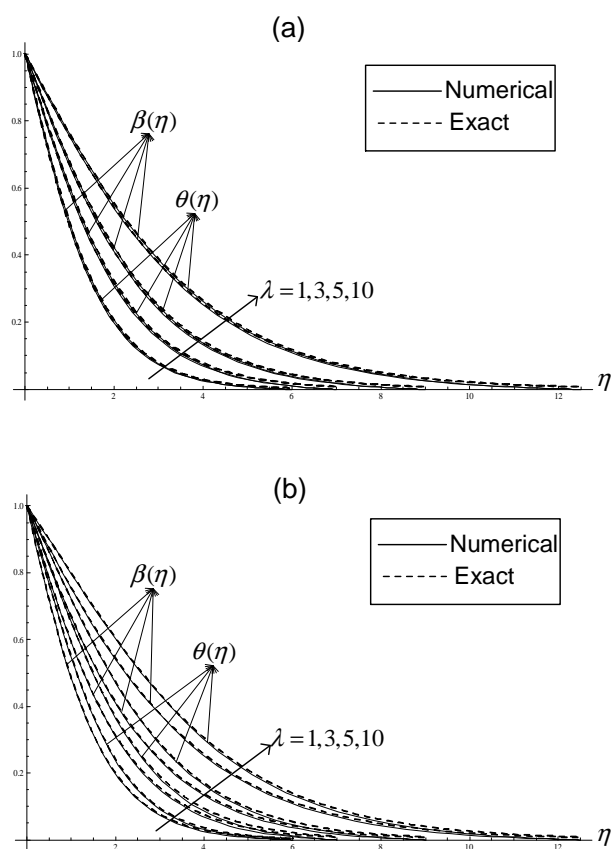


Fig. 7: Exact (dotted line) and numerical (solid line) solutions for $\beta(\eta)$ and $\theta(\eta)$ at $Nb = 0.1$, $Le = Pr = 1$ and $\lambda = 0, 1, 3, 10$ for (a) $Nb = 0.1$ and (b) $Nb = 0.5$.

4.3 Case 3: at $Nb = 0$

In this case, the system (7–8) reduces to a single boundary value problem for θ while the boundary value problem for β becomes ill-posed and is of no physical significance. The BVP for θ becomes

$$\theta''(\eta) + Pr \varepsilon (1 - e^{-\varepsilon\eta}) \theta'(\eta) = 0, \quad (35)$$

where $\theta(0) = 1$ and $\theta(\infty) = 0$. The exact solution of the current case is given as

$$\theta(\eta) = \frac{\Gamma(Pr) - \Gamma(Pr, Pr e^{-\varepsilon\eta})}{\Gamma(Pr) - \Gamma(Pr, Pr)}. \quad (36)$$

Differentiating (36) w.r.t η , we get the reduced Nusselt number as

$$Nur = \frac{\varepsilon(Pr/e)^{Pr}}{\Gamma(Pr) - \Gamma(Pr, Pr)}. \quad (37)$$

5 Conclusion

New theoretical and numerical investigations have been conducted in this paper for studying a system of ordinary differential equations describing the slip effect on the boundary layer flow of nanofluids flow with heat transfer. The theoretical analysis resulted in a set of exact solutions, in terms of exponential, Gamma, and incomplete Gamma functions, at some values of the studying physical parameters; Nt , Nb , Pr and Le . In addition, the numerical results, achieved by using the ChPDM technique, confirm its ability for studying the similar problems with high trust; even if the exact solutions are not available.

References

- [1] T. Altan, S. Oh, H. Gegel, Metal Forming Fundamentals and Applications, American Society of Metals, Metals Park, OH, (1979).
- [2] M.V. Karwe, Y. Jaluria, Numerical simulation of thermal transport associated with a continuous moving flat sheet in materials processing, ASME J. Heat Transfer, **113**, 612–619 (1991).
- [3] V. Kumaran, A. Vanav Kumar, I. Pop, Transition of MHD boundary layer flow past a stretching sheet, Commun. Nonlinear Sci. Numer. Simulat., **15**, 300–311 (2010).
- [4] S. U. S. Choi, Enhancing thermal conductivity of fluids with nanoparticles, The Proceedings of the 1995 ASME International Mechanical Engineering Congress and Exposition, San Francisco, USA, ASME, FED 231/MD, **66**, 99–105 (1995).
- [5] S. U. S. Choi, Z. G. Zhang, W. Yu, F. E. Lockwood, E. A. Grulke, Anomalous thermal conductivity enhancement in nanotube suspensions, Appl. Phys. Lett., **79**, 2252–2254 (2001).
- [6] H. Masuda, A. Ebata, K. Teramae, N. Hishinuma, Alteration of thermal conductivity and viscosity of liquid by dispersing ultra-fine particles (Dispersion of g-Al₂O₃, SiO₂, and TiO₂ ultra-fine particles), Netsu Bussei, **7**, 227–233 (1993).
- [7] S. Lee, S. U. S. Choi, S. Li, J.A. Eastman, Measuring thermal conductivity of fluids containing oxide nanoparticles, Trans. ASME, J. Heat Transfer, **121**, 280–289 (1999).
- [8] Y. Xuan, Q. Li, Heat transfer enhancement of nanofluids, Int. J. Heat Fluid Flow, **21**, 58–64 (2000).
- [9] Y. Xuan, W. Roetzel, Conceptions for heat transfer correlation of nanofluids, Int. J. Heat Mass Transfer, **43**, 3701–3707 (2000).
- [10] D. A. Nield, A. V. Kuznetsov, The Cheng–Minkowycz problem for natural convective boundary layer flow in a porous medium saturated by a nanofluid, Int. J. Heat Mass Transfer, **52**, 5792–5795 (2009).
- [11] A. V. Kuznetsov, D. A. Nield, Natural convective boundary-layer flow of a nanofluid past a vertical plate, Int. J. Therm. Sci., **49**, 243–247 (2010).
- [12] W. A. Khan, I. Pop, Boundary-layer flow of a nanofluid past a stretching sheet, Int. J. Heat Mass Transfer, **53**, 2477–2483 (2010).

- [13] N. Bachok, A. Ishak, I. Pop, Boundary-layer flow of nanofluids over a moving surface in a flowing fluid, *Int. J. Therm. Sci.*, **4**, 1663–1668 (2010).
- [14] E. H. Aly, A. Ebaid, New exact solutions for boundary-layer flow of a nanofluid past a stretching sheet, *J. Comput. Theor. Nanosci.*, **10**, 25912594 (2013).
- [15] M. Majumder, N. Chopra, R. Andrews, B.J. Hinds, Nanoscale hydrodynamics: enhanced flow in carbon nanotubes, *Nature*, **438**, 44 (2005).
- [16] A. Noghrehabadi, R. Pourrajab, M. Ghalambaz, Effect of partial slip boundary condition on the flow and heat transfer of nanofluids past stretching sheet prescribed constant wall temperature, *Int. J. Therm. Sci.*, **54**, 253–261 (2012).
- [17] M. Gad-el-Hak, The fluid mechanics of macrodevices—the Freeman scholar lecture, *J. Fluids Eng.*, **121**, 5–33 (1999).
- [18] R. A. Van Gorder, E. Sweet, K. Vajravelu, Nano boundary layers over stretching surfaces, *Commun. Nonlinear Sci. Numer. Simulat.*, **15**, 1494–1500 (2010).
- [19] E. H. Aly, A. Ebaid, On the exact analytical and numerical solutions of nano boundary-layer fluid flows, *Abst. Appl. Anal.*, **2012**, Article ID 415431, 22 pages, (2012).
- [20] A. Ebaid, N. Abd Elazem, On the exact solutions of a nano boundary layer problem using the simplest equation method, *Phys. Scr.*, **84**, 065005, (2011).
- [21] E. H. Aly, M. Benlalsen, M. Guedda, Similarity solutions of a MHD boundary-layer flow past a continuously moving surface, *Int. J. Eng. Sci.*, **45**, 486–503 (2007).
- [22] M. Guedda, E. H. Aly, A. Ouahsine, Analytical and ChPDM analysis of MHD mixed convection over a vertical flat plate embedded in a porous medium filled with water at 4°C, *Appl. Math. Model.*, **35**, 5182–5197 (2011).
- [23] E. H. Aly, A. Ebaid, New theoretical and numerical solutions for mixed convection boundary-layer nanofluid flow along an inclined plate embedded in a porous medium, *J. Appl. Math.*, in the special issue: Mathematical and Numerical Modeling of Flow and Transport, **2013**, Article ID 219486, 7 pages, (2013).
- [24] E. H. Aly, M. A. Hassan, Suction and injection analysis of MHD nano boundary-layer over a stretching surface through a porous medium with partial slip boundary condition, *J. Comput. Theor. Nanosci.*, **11**, 827-839 (2014)
- [25] E. M. E. Elbarbary, S. M. El-Sayed, Higher order pseudospectral differentiation matrices, *Appl. Numer. Math.*, **55**, 425–438 (2005).

Loughborough University in modeling for Chemical Engineering and handled this project successfully before the official deadline. He is mainly interested in Fluid Mechanics and its Applications in Science.



Abdelhalim Ebaid

is associate professor at university of Tabuk, Faculty of Science, Department of Mathematics. He was born on August 4 1972 in Cairo, Egypt. He received his B.Sc. from the Department of Mathematics, Faculty of Education of Ain Shams

University in 1994. His M.Sc. in Differential Equations was from Ain Shams University in 2003 and his Ph.D. in Differential Equations was from Ain Shams University in 2007. He interested in the analytical and numerical solutions of applied differential equations.



Nader Abd Elazem

is Assistant professor at university of Tabuk, Faculty of Science, Department of Mathematics. He was born on September 3 1969 in Cairo, Egypt. He received his B.Sc. from the Department of Mathematics, Faculty of Education of Ain Shams

University in 1991. His M.Sc. in Partial Differential Equations was from Ain Shams University in 2003 and his Ph.D. in Partial Differential Equations was from Ain Shams University in 2009. He interested in the Computational Fluids Mechanic.



Emad H. Aly, In 2003 and to study towards his M.Sc. under the supervision of Professor Derek Ingham in Computational Fluid Mechanics, Emad Aly has been awarded a scholarship from King Faisal Foundation (SA), Leeds University (UK) and Royal Society of London.

He has then got a Ph.D. studentship from Loughborough University (UK) in Applied Mathematics for Engineering and completed it in 2007. At the same year, Emad has also received a Postdoctoral Research Associate from